Near-infrared luminescence of bismuth in fluorine-doped-core silica fibres

A.P. Bazakutsa[1,*] and K.M. Golant[1]

[1]*Kotel'nikov Institute of Radio-engineering and Electronics of RAS, Russian Federation*
[*]*abazakutsa@gmail.com*

Abstract: Photoluminescence spectra and decay kinetics of bismuth inclusions in silica optical fibres containing fluorine additive in the core glass are studied in the vicinity of a wavelength of 1420 nm at temperatures of 80–900 K under a continuous wave (CW) and a pulsed diode laser pump at a wavelength of 808 nm. At high fluorine concentration and low temperatures, luminescence decay kinetics becomes essentially bi-exponential, typical lifetimes being 720 and 1200 μs. Hydrogen and deuterium loading at pressures of up to 125 bar leads to a decrease of the steady-state luminescence intensity and lifetime. We attribute this to the appearance of an energy transfer bridge from bismuth clusters to vibrational degrees of freedom of diatomic molecules. It is found that in the presence of H_2 or D_2 molecules experiencing random walking in silica, luminescence decay kinetics stop following a single exponential function even in fluorine-free silica-core fibre, deviation from the single exponent being greater at higher temperatures. The induced quenching rate increases with the increase of temperature as well and is greater for H_2 molecules. All conditions being equal, the equilibrium concentration of hydrogen molecules is greater in heavily fluorinated silica. At temperatures below ~250 K, the presence of dissolved molecules has no effect, which speaks for the primary importance of having rotational degrees of freedom of migrating interstitial diatomic molecules in an excited state for effective quenching of bismuth electronic excitations. It is found that the influence of dissolved deuterium is weaker than that of hydrogen. We attribute this feature to a greater angular momentum of the D_2 molecule and correspondingly smaller energy of the molecule's rotational quantum. The results of the experiments show that bismuth clusters mainly located in voids of the silica network, rather than bismuth point defects, are responsible for near-infrared luminescence.

OCIS codes: (160.2290) Fiber materials; (160.2540) Fluorescent and luminescent materials; (060.2280) Fiber design and fabrication.

References and links

1. Y. Fujimoto and M. Nakatsuka, "Infrared luminescence from bismuth-doped silica glass," Jpn. J. Appl. Phys. **40**(Part 2, No. 3B), L279–L281 (2001).
2. E. M. Dianov, "Amplification in extended transmission bands using bismuth-doped optical fibers," J. Lightwave Technol. **31**(4), 681–688 (2013).
3. M. Peng, G. Dong, L. Wondraczek, L. Zhang, N. Zhang, and J. Qiu, "Discussion on the origin of NIR emission from Bi-doped materials," J. Non-Cryst. Solids **357**(11-13), 2241–2245 (2011).
4. B. Kusz, D. Pliszka, M. Gazda, R. S. Brusa, K. Trzebiatowski, G. P. Karwasz, A. Zecca, and L. Murawski, "Structural studies of bismuth nanocrystals embedded in SiO_2 or GeO_2 matrices," J. Appl. Phys. **94**(11), 7270–7275 (2003).
5. T. Wakabayashi, M. Tomioka, Y. Wada, Y. Miyamoto, J. Tang, K. Kawaguchi, S. Kuma, N. Sasao, H. Nanjo, S. Uetake, M. Yoshimura, and I. Nakano, "Observation of new near-infrared emission band systems of small bismuth clusters in solid neon matrix," Eur. Phys. J. D **67**(2), 36 (2013).

#227047 - $15.00 USD Received 18 Nov 2014; revised 19 Jan 2015; accepted 22 Jan 2015; published 6 Feb 2015

6. J. Toudert, R. Serna, and M. J. de Castro, "Exploring the optical potential of nano-bismuth: tunable surface plasmon resonances in the near ultraviolet-to-near infrared range," J. Phys. Chem. C **116**(38), 20530–20539 (2012).
7. A. Trukhin, J. Teteris, A. Bazakutsa, and K. Golant, "Intra-center and recombination luminescence of bismuth defects in fused and unfused amorphous silica fabricated by SPCVD," J. Non-Cryst. Solids **363**, 187–192 (2013).
8. I. A. Bufetov, K. M. Golant, S. V. Firstov, A. V. Kholodkov, A. V. Shubin, and E. M. Dianov, "Bismuth activated alumosilicate optical fibers fabricated by surface-plasma chemical vapor deposition technology," Appl. Opt. **47**(27), 4940–4944 (2008).
9. K. M. Golant, A. P. Bazakutsa, O. V. Butov, Yu. K. Chamorovskij, and A. V. Lanin, "Bismuth-activated silica-core fibres fabricated by SPCVD," presented at ECOC 2010 – 36th European Conference and Exhibition on Optical Communication, Turin, Italy, 19–23 September 2010.
10. A. P. Bazakutsa, O. V. Butov, and K. M. Golant, "Influence of hydrogen loading on active fibers," in *Optical Fiber Communication Conference*, Poster Session II (**JTh2A**), Anahaim, USA, 17–21 March 2013.
11. A. P. Bazakutsa, O. V. Butov, E. A. Savel'ev, and K. M. Golant, "Specific features of IR photoluminescence of bismuth doped silicon dioxide synthesized by plasmachemical method," J. Commun. Technol. Electron. **57**(7), 743–750 (2012).
12. K. M. Golant, "Bulk silicas prepared by low pressure plasma CVD: formation of structure and point defects," in *Defects in SiO_2 and Related Dielectrics: Science and Technology*, G. Pacchioni, L. Skuja, D. Griscom, eds. (Kluwer Academic Publishers, 2000), pp. 427–452.
13. I. A. Bufetov, K. M. Golant, S. V. Firstov, A. V. Kholodkov, A. V. Shubin, and E. M. Dianov, "Bismuth activated alumosilicate optical fibers fabricated by surface-plasma chemical vapor deposition technology," Appl. Opt. **47**(27), 4940–4944 (2008).
14. J. W. Fleming and D. L. Wood, "Refractive index dispersion and related properties in fluorine doped silica," Appl. Opt. **22**(19), 3102–3104 (1983).
15. C. L. Liou, L. A. Wang, M. C. Shih, and T. J. Chuang, "Characteristics of hydrogenated fiber Bragg gratings," Appl. Phys., A Mater. Sci. Process. **64**(2), 191–197 (1997).
16. J. Stone, "Interactions of hydrogen and deuterium with silica optical fibers: a review," J. Lightwave Technol. **5**(5), 712–733 (1987).
17. R. Kohlrausch, "Theorie des elekirkhen Riickstundes in der Leidener Flasche," Poggendorff's Ann. Phys. **167**(1), 56–82 (1854).
18. K. Médjahdi, A. Boukenter, and Y. Ouerdane, "Collisional deactivation mechanism of luminescence in hydrogen-loaded Ge-doped fibers," J. Chem. Phys. **123**(21), 214701 (2005).
19. C. M. Hartwig, "Raman scattering from hydrogen and deuterium dissolved in silica as a function of pressure," J. Appl. Phys. **47**(3), 956–959 (1976).
20. V. S. Efimchenko, V. K. Fedotov, M. A. Kuzovnikov, A. S. Zhuravlev, and B. M. Bulychev, "Hydrogen solubility in amorphous silica at pressures up to 75 kbar," J. Phys. Chem. B **117**(1), 422–425 (2013).
21. X. Xu, W. Yang, C. Song, J. Liu, and L. Lin, "Hydrogen separation by zeolite membranes," Prepr. Pap. - Am. Chem. Soc., Div. Fuel Chem. **48**(1), 284–285 (2003).
22. A. I. Burshtein, "Energy quenching kinetics beyond the rate concept," J. Lumin. **93**(3), 229–241 (2001).

1. Introduction

Fujimoto and Nakatsuka's finding of near-infrared luminescence in bismuth-doped silica [1] has inspired the study of this dopant as an activator for fibre lasers and amplifiers. Its importance for the telecommunications wavelengths band ranging from 1.1 to 1.5 μm uncovered by alternative activators adds much to study the bismuth-doped fibres. Certain information on the modern state of research in this field can be found in review articles [2, 3].

By contrast to rare earth dopants, in which optical gain is achieved due to electron transitions between steady state terms of ***f***-electron shells in a triply ionized dopant, electron transitions responsible for photoluminescence and lasing in the case of bismuth activators are not quite clear yet. The known trend of bismuth to form metallic clusters hinders the search for an adequate model of bismuth activators embedded in a silica network [4]. The formation of clusters leads to a multiplicity of polyatomic bismuth aggregates able to contribute to near-infrared luminescence. The experiments described in [5] are an example that unambiguously illustrates the ability of bismuth clusters to emit in the near-infrared band. Clusters studied in [5] are formed by the condensation of bismuth vapours in a flow of inert neon on a copper substrate cooled to a liquid helium temperature. It is clear that the formation of covalent and/or ionic bonds in solid composites obtained in this way is possible between bismuth atoms only. Therefore the luminescence observed is due to electron transitions between separately located bismuth atoms, dimers, trimers, and tetramers as well as many other atomic clusters frosted in a host composed of atoms of the inert gas. A larger size bismuth clusters

#227047 - $15.00 USD Received 18 Nov 2014; revised 19 Jan 2015; accepted 22 Jan 2015; published 6 Feb 2015

embedded in various dielectric media can function as surface plasmon resonators as well. The spectrum of resonance bands varies from the UV to the near infrared one [6].

Bismuth's tendency to form metallic clusters in SiO_2 is caused by a lack of the necessary conditions for the formation of a strong chemical bonding between bismuth and oxygen inside the silica network. The absence of such bonding is indirectly confirmed by the experiments on temperature dependence of Bi-doped silica luminescence excited by deep ultraviolet light. As shown in [7], bismuth cannot serve as a recombination trap for electron–hole pairs excited in amorphous silicon dioxide host as a result of absorption of UV photons. This indicates that there may be a potential barrier between the electron structure of the host (amorphous SiO_2) on the one hand and bismuth inclusions on the other.

Clustering of bismuth in the SiO_2 network in the form of metallic inclusions differs fundamentally from that of rare earth dopants, which at moderate concentrations tend to form inclusions constituting crystals of corresponding oxides. Herewith, in the case of rare earth activators, breakdown of luminescence characteristics caused by co-operative effects notably occurs at concentrations greater than $\sim 10^{20}$ cm^{-3}, while for bismuth it already becomes significant at $\sim 10^{18}$ cm^{-3} [8]. This means that the mobility of bismuth during high-temperature silica processing typical for optical fibre technologies is much greater than the mobility of the rare earth ions. For this reason, the formation of bismuth clusters in the process of melting of initially uniform bismuth-doped amorphous silicon dioxide takes place at a greater rate.

Taking into account the above-mentioned facts, one can suppose that a modification of the silica network can significantly influence the structure and frame of bismuth inclusions in silica and thus substantially affect the near-infrared luminescence. It is modification of the silica network which most likely causes sensitivity of the luminescence spectra to aluminum and phosphorous dopants [9]. From this viewpoint, partial substitution of oxygen with fluorine seems to be an effective means of such modification as well.

The aim of this work is to study experimentally how the luminescence properties of bismuth inclusions depend on the addition of fluorine in the silica network. Experiments are carried out with the help of bismuth-doped multimode silica fibres with different fluorine contents in the core and heavily fluorine-doped silica as a light-reflecting cladding. The fibres were specially fabricated for this purpose. The spectra and kinetics of luminescence pumped at a wavelength of 808 nm are measured at temperatures ranging from 77 to 900 K within the 850–1600-nm wavelength band. Measurements at different temperatures are performed in ambient air and in hydrogen or deuterium environments in a chamber under a pressure of 100 bar. Experimenting with hydrogen and deuterium allows us to observe changes of luminescence characteristics of bismuth inclusions as affected by the Brownian motion of H_2 and D_2 molecules entering the silica network as a result of diffusion. Earlier it was shown [10] that luminescence quenching caused by migrating hydrogen molecules is most effective for bismuth inclusions as compared to other activators: random walking of interstitial molecules predominantly occurs inside the voids of the amorphous silicon dioxide network exactly where most of the bismuth inclusions are located.

The use of hydrogen isotopes to probe luminescence quenching by randomly walking diatomic molecules fits due to the rather big diffusion coefficients in SiO_2 and consequently the rather short time necessary for equilibration of the concentration in a glass network even at room temperature. Within this framework, the use of samples in the form of a thin optical fibre ~125 microns in diameter provides a significant advantage for the execution of measurements.

The effect of deactivation of bismuth aggregates' excitations by migrating hydrogen and deuterium molecules is used in the current research as a tool which could elucidate the origin and position of bismuth inclusions in the amorphous silicon dioxide network modified with fluorine. The present work is performed as an extension of the results of [11], where the luminescence of bismuth-doped silica glasses is studied as a function of temperature. We also rely on the results of [10], in which the effect of deactivation of excited Er^{3+}, Yb^{3+}, and Nd^{3+}

#227047 - $15.00 USD Received 18 Nov 2014; revised 19 Jan 2015; accepted 22 Jan 2015; published 6 Feb 2015

ions by the motion of interstitial molecular hydrogen dissolved in silica fibres was demonstrated for the first time, and it was shown that the abovementioned effect manifests itself much more strongly in the case of near-infrared luminescence of bismuth.

2. Fibre samples

Polymer-coated silica optical fibres are used in the experiments. The fibres' refractive index profile is shown in Fig. 1. The light-guiding structure consists of a silica core containing bismuth and different amounts of fluorine additive covered by a heavily fluorine-doped silica light-reflecting cladding. As can be seen from Fig. 1, the fibres are multimode with a numerical aperture of NA ~0.1. The fibres' outer and core diameters are 125 μm and ~20 μm respectively. All fibres are drawn from preforms fabricated by the SPCVD method [12]. For more details on the application of this method to the synthesis of bismuth-doped silica, see [13].

Table 1 summarizes the key parameters of the fibres. Sample #1 contains no fluorine additive in the core, whilst samples #2 and #3 have different fluorine contents, which is seen from Fig. 1 as well. Note that high-temperature treatment in the collapsing process of the substrate tube together with the layers deposited by SPCVD, which is intrinsic to the fabrication of fibre preforms, leads to a partial outcome of bismuth and fluorine from the deposited layers, which brings a peculiarity of the refractive index profile that is most noticeable in sample #3 (Fig. 1).

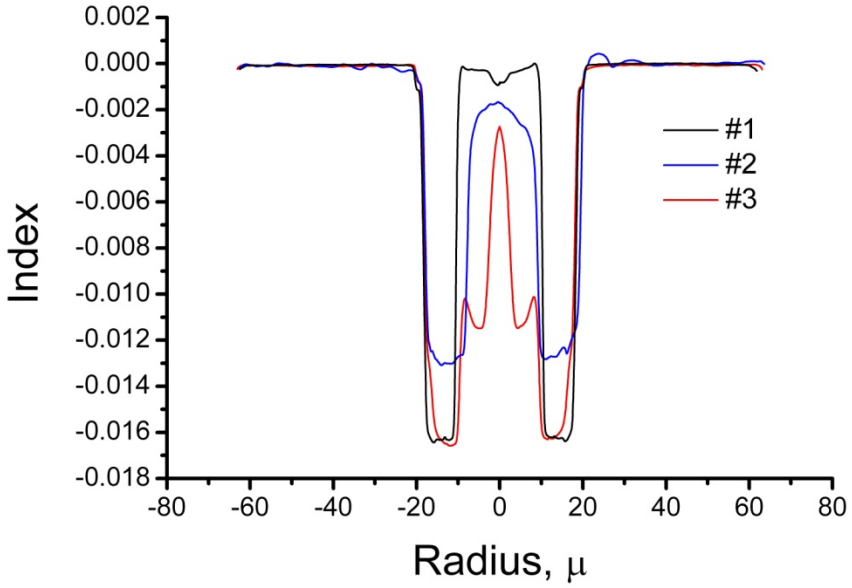

Fig. 1. Refractive index profiles of the fibres under study.

Table 1. Key parameters of the fibres used in the experiments

Sample number	Absorption coefficient at 808-nm wavelength, dB/m	F concentration in the fibre core, wt.%
#1 (no F)	19.7	0
#2 (low F)	35.8	0.52
#3 (high F)	15.0	3.12

The bismuth content in all of the samples is below the sensitivity limit of a standard x-ray microprobe analyser. A certain criterion for rough estimation of bismuth contents in different

#227047 - $15.00 USD Received 18 Nov 2014; revised 19 Jan 2015; accepted 22 Jan 2015; published 6 Feb 2015

fibre samples, however, is a peak absorption at a wavelength of 808 nm (see also Fig. 3). The fluorine content in the fibre core can be estimated from the refractive index profile [14].

3. Photoluminescence measurement technique

Luminescence spectra and kinetics are recorded on pumping of a piece of a fibre by 808-nm wavelength radiation from a laser diode launched in the fibre core through the port ‘a’ of a wideband (700–1500 nm) directional coupler (Fig. 2). A fibre line with a built-in section of bismuth-doped fibre ~20 cm in length is connected to port ‘c’ of the coupler. The bismuth-doped fibre section is passed through a chamber filled with hydrogen or deuterium at a pressure of up to 100 bar. The opposite vacant end of the fibre line, which is terminated by an oblique cut, is immersed in an index-matched liquid to reduce back-scattered pump light.

The hydrogen chamber constitutes a stainless steel tube section with an outer diameter of 6 mm and wall thickness of 1 mm connected to a buffer capacity. The temperature of the tube section with the sealed bismuth-doped fibre inside is set and stabilized to an accuracy of ~6 K within the range of 300–900 K. The buffer capacity, which is maintained at room temperature, keeps the pressure in the chamber unchanged while the tube section with the fibre changes temperature.

Photoluminescence is excited by a laser diode at a wavelength of 808 nm in CW or pulsed periodic (30-ms meander) regimes for recording of luminescence spectra and decay kinetics, respectively. The average pump power delivered to the fibre does not exceed ~1 mW. The luminescence signal is brought out through the port ‘b’ of the coupler and is fed to an InGaAs photodiode through a notch filter, rejecting the rest of the back-scattered pump light. A photodiode is connected to a Tektronics DPO3012 oscilloscope to record the luminescence decay kinetics. The response time of the pump modulation and photo-receiver systems is less than 50 μs. To measure the luminescence spectra, pump radiation is launched directly in the fibre and the luminescence signal is recorded from the opposite end of the fibre with the help of a HP86142A spectrum analyser.

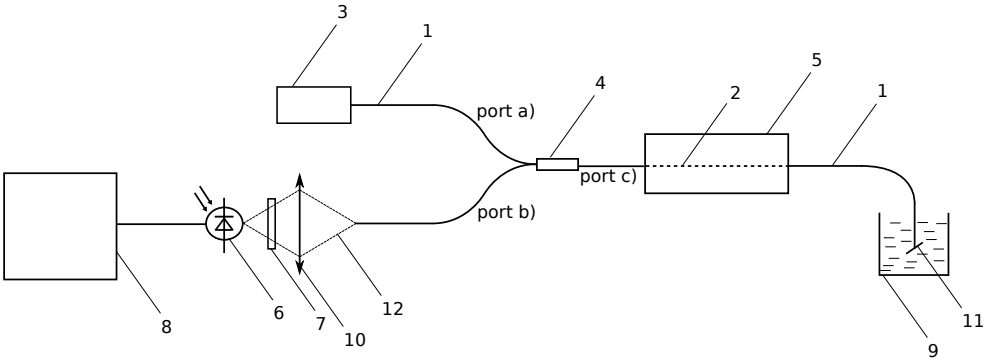

Fig. 2. Measurement design for photoluminescence decay kinetics in a fibre placed in the gas saturation chamber: 1 – delivery fibre, 2 – active fibre, 3 – pump laser diode, 4 – directional fibre coupler, 5 – chamber for gas loading, 6 – photo-receiver, 7 – notch filter, 8 – oscilloscope, 9 – bath with immersion liquid, 10 – lens, 11 – oblique fibre cut.

Measurements are arranged as follows. First of all, luminescence spectra and decay kinetics are recorded at different temperatures in the fibre kept in air. Then hydrogen or deuterium fills the chamber, and photoluminescence characteristics are measured at regular intervals as gas molecules are entering the fibre core. During this procedure, the temperature of an active fibre in the chamber is maintained at about 403 K in order to speed up the in-diffusion process. The concentration of interstitial molecules in the core of the fibre after staying for some time in the chamber with gas is estimated according to a known diffusion formula [15]. As soon as the equilibrium concentration is reached, the temperature in the chamber is slowly raised to about 873 K. Luminescence characteristics are recorded on

#227047 - $15.00 USD Received 18 Nov 2014; revised 19 Jan 2015; accepted 22 Jan 2015; published 6 Feb 2015

heating every 50 °C. The dependence of solubility on temperature is taken into account when calculating the equilibrium values of concentrations of H_2 and D_2 molecules [16].

Measurements of hydrogen- and deuterium-loaded fibres at lower temperatures are carried out in the course of cooling of fibres extracted from the gas chamber in the liquid nitrogen vapour flow. The permanent cooling rate is about 10 K/min. Note that in this part of the experiment the temperature of the fibre never exceeds 403 K.

4. Results

4.1 Dependence on temperature during heating in air

Figure 3(a) shows the pristine absorption spectra measured in the fibres of different lengths by the cut-back method in the spectral band of 250–1600 nm. It is seen that all three samples have intense absorption bands centred at 808 and 1420 nm, and the corresponding absorption coefficients of these bands for different samples are of the same order of magnitude. This means that the concentrations of bismuth inclusions responsible for absorption in these spectral bands do not vary significantly. The normalized luminescence spectra presented in Fig. 3(b) give support to the abovementioned conclusion as well (there is a small difference in luminescence intensity only, but not in the 1420 nm band shaping).

A significant difference between the absorption spectra, however, is observed in the visible and UV bands as well as in the wavelength range of 900–1100 nm. It can be seen, in particular, that in the presence of fluorine the absorption bands at wavelengths of 940–1000 nm are sharper, and very different spectra are observed at wavelengths of 250–500 nm. In particular, an extra maximum appears for sample #3 at a wavelength of about 300 nm (note the logarithmic scale).

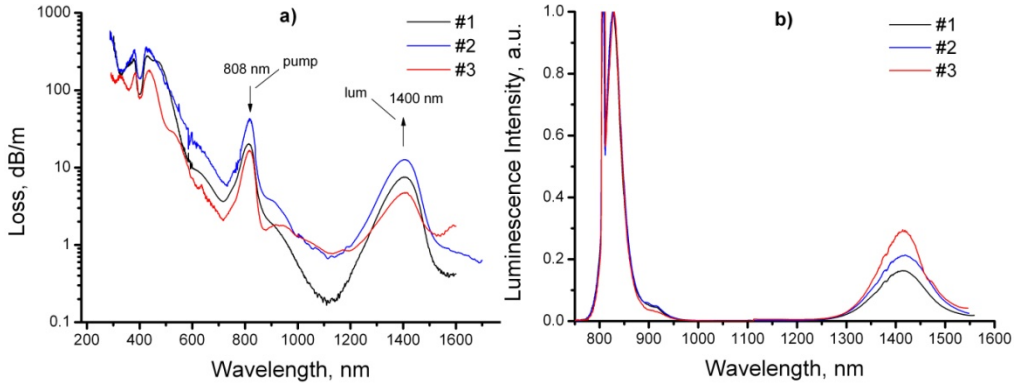

Fig. 3. Absorption (a) and luminescence (b) spectra of the fibres under study.

Figure 4 shows the near-infrared luminescence spectra measured in all samples at different temperatures in the air environment. The intensity of the band at ~830 nm decreases with increasing temperature, but the band at ~1420 nm has the opposite tendency.

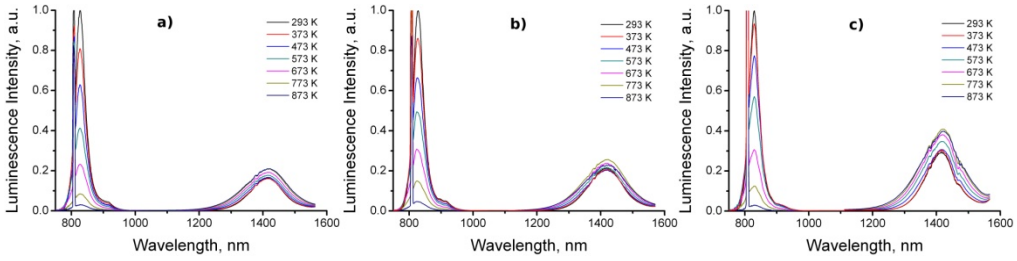

Fig. 4. Luminescence spectra of samples #1 – (a), #2 – (b), and #3 – (c) recorded at different temperatures in fibres kept in air.

#227047 - $15.00 USD Received 18 Nov 2014; revised 19 Jan 2015; accepted 22 Jan 2015; published 6 Feb 2015

Figure 5 shows the luminescence decay curves of the 1420-nm wavelength peak obtained for each fibre sample at three different temperatures.

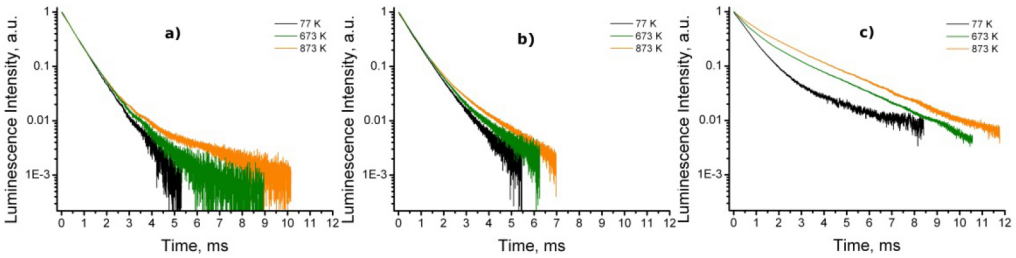

Fig. 5. Luminescence decay curves of samples #1 – (a), #2 – (b), and #3 – (c) obtained at temperatures of 77, 673, and 873 K.

One can see that with increasing temperature, the shapes of the decay curves change differently for samples #1 to #3; however a common tendency of the decay rate to slow down at higher temperatures takes place. The increase in the lifetime correlates with the abovementioned growth of the intensity peak at a wavelength of 1420 nm in the spectra of the steady-state luminescence. Note that the decay curve shape for fluorine-free (#1) and slightly fluorinated (#2) core fibres is more weakly dependent on temperature compared to the one with a greater fluorine content in the core (#3). It is notable that for this sample the greatest acceleration of luminescence decay rate with decreasing temperature is observed.

Good fitting for the measured luminescence decay curves gives a bi-exponential dependence. Figure 6 shows the best-fitted time constants and pre-exponential factors for decay curves at different temperatures approximated in such a way. It is seen that a longer-living component manifests itself only at temperatures greater than ~400 K, when its contribution to the decay curve increases significantly. According to Fig. 6(1b)-6(3b), the observed deceleration in the decay rate with increasing temperature can be interpreted as a competing contribution of two exponents, where heating leads to a shift of the balance toward the longer-living one. Both time constants are weakly dependent on temperature.

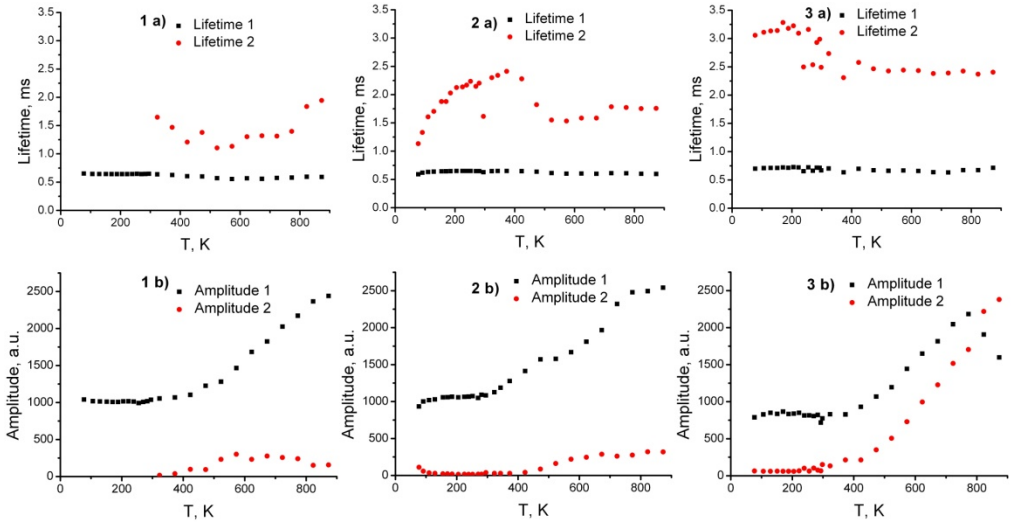

Fig. 6. Dependences of time constants (1a) – (3a) and corresponding pre-exponential factors (1b) – (3b) on temperature in the range of 89 – 873 K. Plots are labelled by numbers corresponding to samples.

#227047 - $15.00 USD Received 18 Nov 2014; revised 19 Jan 2015; accepted 22 Jan 2015; published 6 Feb 2015

4.2 Effects of hydrogen and deuterium loading

As soon as hydrogen or deuterium enters the chamber with the fibre, in-diffusion of molecules starts to occur. Figure 7 illustrates the dependence of the concentration of H_2 molecules reaching the core of different optical fibres used in our experiments on the duration of stay in the chamber with hydrogen at room temperature. The relative concentration of H_2 molecules is determined by the intensity of the absorption peak centred at a wavelength of 1240 nm measured in fibre sections 9.4 m in length placed in the chamber filled with hydrogen at a pressure of 90 bar. This experiment lasted two weeks in order to achieve the maximum (saturating) hydrogen concentration in the fibre core. According to Fig. 7, the solubility of molecular hydrogen in the fluorine-modified silica network is slightly greater, which indirectly indicates the porosity of the glass network.

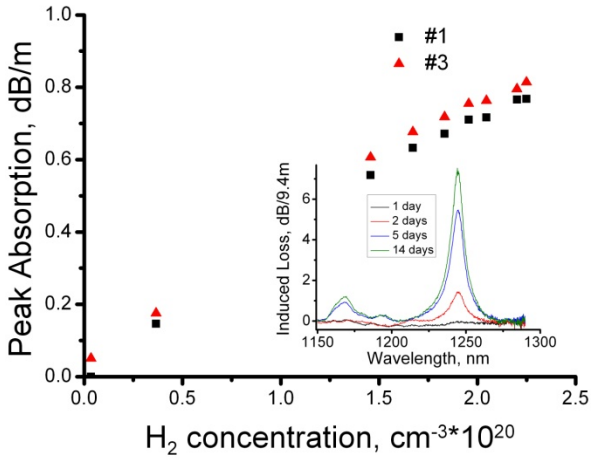

Fig. 7. Dependences of 1240-nm wavelength-peak absorption coefficients on hydrogen concentration in the core for samples #1 and #3. Inset: absorption spectrum evolution caused by penetration of hydrogen molecules in the core of fibre #1 upon ageing it in the chamber filled with hydrogen at a pressure of 90 bar at room temperature.

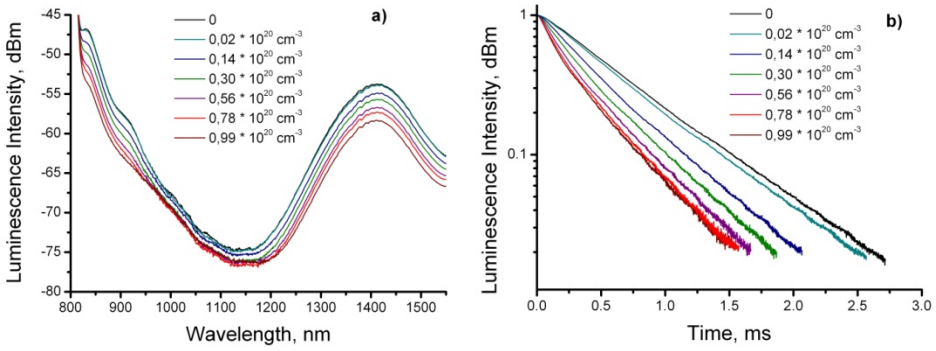

Fig. 8. Luminescence spectra (a) and decay kinetics (b) of sample #1 at different hydrogen concentrations in the fibre core.

The luminescence spectra and decay kinetics variations in the course of penetration of hydrogen molecules in the glass of the core of fibre #1 at a temperature of 473 K are shown in Fig. 8. No qualitative difference in the dynamics of luminescence spectra and decay kinetics

#227047 - $15.00 USD Received 18 Nov 2014; revised 19 Jan 2015; accepted 22 Jan 2015; published 6 Feb 2015

evolution for different samples in the processes of their saturation with H_2 and/or D_2 molecules is revealed in the course of the experiments. It is seen that the intensity and lifetime of the luminescence decrease. It is important to note that with an increase of the hydrogen concentration in the glass of the fibre core, the deviation of the single exponential decay for samples #1 and #2 is already observed at room temperature. The best fitting results for these decay curves provide the stretched exponential or Kohlrausch function [17]:

$$I(\mathrm{t}) = I_0 * \exp\left(\left(-\frac{t}{\tau}\right)^{\beta}\right), \qquad (1)$$

where I(t) is the luminescence intensity, t is time, I_0 is intensity at $t = 0$, τ is the factor having the dimension of time, which we shall hereinafter call 'lifetime' for convenience, and β is the factor characterizing the stretching of the exponent. Obviously, at $\beta = 1$, function (1) degenerates into the conventional exponent.

The observed impact of H_2 and/or D_2 loading on luminescence is reversible. This means that the intensity and the decay kinetics of luminescence return to a previous condition after the escape of dissolved molecules from the fibre in the air.

In paragraph 2.1 we have demonstrated that luminescence decay in the pristine fibres is bi-exponential. Whereas hydrogen loading leads to a "stretching" of the exponent showing the decay, it would make sense to suppose that both exponents intrinsic to the decay process should be stretched. However, according to Fig. 6, the proportion of the long-living component in the luminescence decay kinetics for samples #1 and #2 does not exceed 10%. For this reason we fitted the decay process in these samples by one stretched exponent. In considering the luminescence decay kinetics of sample #3, one cannot ignore the presence of a long-living component at temperatures exceeding 300 K. At maximum temperatures, the pre-exponential factors for "slow" and "fast" exponents are practically equal (Fig. 6(3b)). However, here again we formally fitted the luminescence decay curves with relation (1) as well as for the other samples. Although the thus-obtained values of τ and β can be rather nominally compared with similar ones for samples #1 and #2, such a comparison nonetheless provides the chance to picture the evolution of complicated luminescence decay kinetics in hydrogen- and deuterium-loaded sample #3 at various temperatures. We shall consider the origin of the stretch exponent in our experiments in more detail in the next paragraph, indicating here only that all luminescence decay curves of hydrogen- and/or deuterium-loaded fibre samples are fitted by the Kohlrausch function (1).

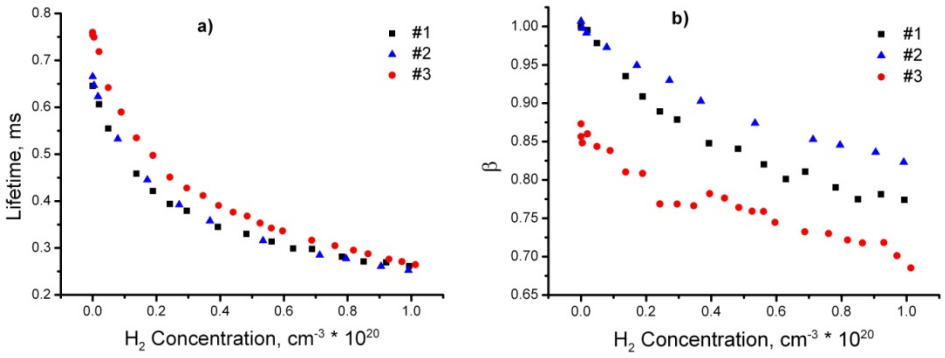

Fig. 9. Dependencies of lifetime (a) and β-factor (b) on the concentration of hydrogen molecules in the fibre cores at 403 K.

#227047 - $15.00 USD Received 18 Nov 2014; revised 19 Jan 2015; accepted 22 Jan 2015; published 6 Feb 2015

Figure 9 illustrates the dependences of the τ- and β-factors on the concentration of dissolved hydrogen for all samples at 493 K. It is seen that violation of the exponential decay expressed in terms of deviation of the β-factor from unity grows with the increase in the dissolved hydrogen concentration and is greatest for sample #3, which contains the maximum fluorine admixture in the core glass. This most likely results from a greater percentage of bismuth located in glass voids and consequently a greater probability that active bismuth clusters will contact migrating gas molecules dissolved in the glass. However, in this sample, deviation of exponential decay ($\beta < 1$) is observed even in the absence of dissolved hydrogen.

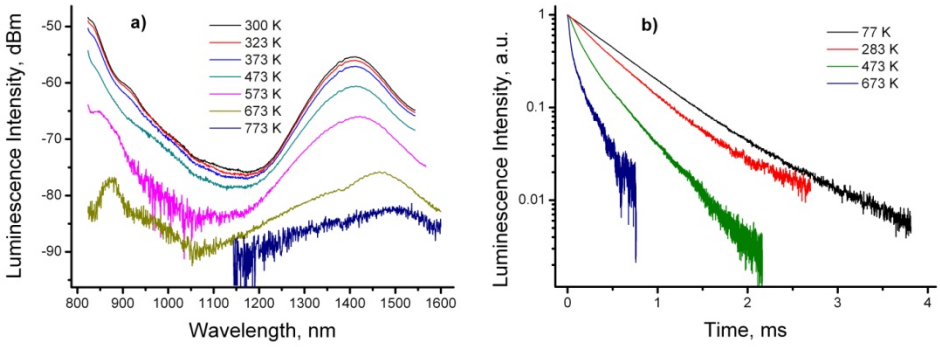

Fig. 10. Luminescence spectra (a) and decay kinetics (b) of hydrogen-loaded sample #1 measured at different temperatures.

The impact of hydrogen molecules dissolved in glass on the luminescence of bismuth inclusions is most clearly observed in the process of temperature increase. Figure 10 illustrates the photoluminescence spectra and kinetics changes caused by temperature variation in hydrogen-loaded sample #1. Similar dependencies are observed in other samples as well. To quantify the luminescence decay kinetics changes in the gas-loaded samples it is convenient to operate with a variable "deactivation rate" instead of "lifetime":

$$Rate = \frac{1}{\tau}, \tag{2}$$

where τ is the measured lifetime. Following [18], we can equate the quenching rate in the form:

$$Rate = \tau_{rad}^{-1} + k(\mathrm{T}) * \mathrm{n}_{gas}(\mathrm{T}), \tag{3}$$

where n_{gas} is the concentration of hydrogen or deuterium molecules, k is the quenching probability per unit time per one molecule in a unit volume, τ_{rad} is the decay time constant in a pristine sample, and T is temperature.

As previously mentioned, the equilibrium concentration of gas molecules dissolved in the glass decreases with the increase of temperature due to a decrease of solubility. Therefore, to correctly estimate the data obtained, we normalize the quenching rate to an equilibrium concentration of gas molecules dissolved in the fibre core, and thus the average contribution of each molecule to the quenching process can be expressed as:

$$k(\mathrm{T}) = \frac{Rate - \tau_{rad}^{-1}}{n_{gas}(\mathrm{T})}. \tag{4}$$

#227047 - $15.00 USD Received 18 Nov 2014; revised 19 Jan 2015; accepted 22 Jan 2015; published 6 Feb 2015

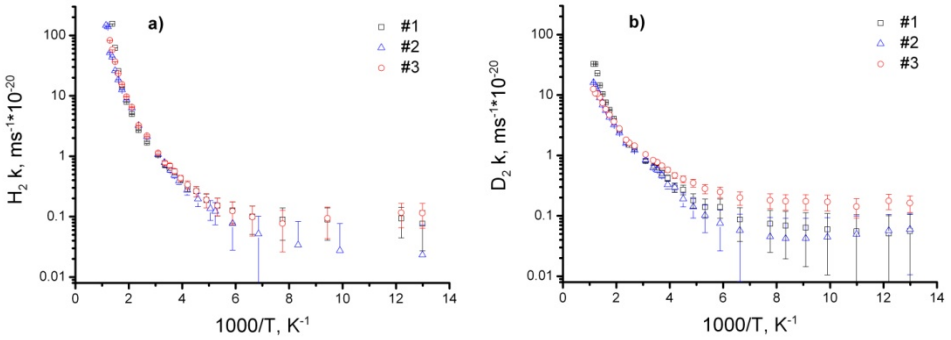

Fig. 11. Dependences of normalized induced quenching rates on temperature for hydrogen- (a) and deuterium- (b) loaded samples #1 to #3. Vertical error bars correspond to statistical errors, calculated in the ordinary way.

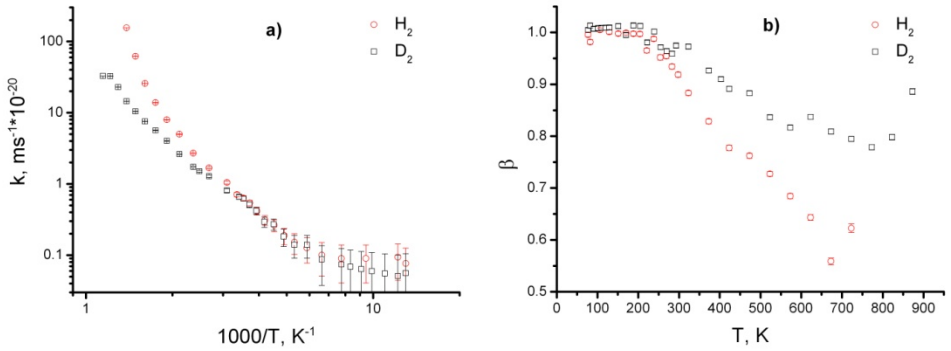

Fig. 12. Normalized quenching rate (a) and β-factor (b) for hydrogen-loaded sample #1 at different temperatures.

Dependences *k(T)* obtained from the measured luminescence decay curves in accordance with relation (4) are depicted in Fig. 11. There are no significant differences between temperature dependences of quenching rates in all gas-loaded samples. However the impacts of hydrogen and deuterium differ greatly (Fig. 12). In particular, hydrogen quenches excitations more effectively than deuterium. This is expressed in a greater activation energy for *k(T)* function in a higher temperature region as well as in a stronger impact of hydrogen on the transfer of the decay to a stretched exponential ($\beta < 1$) form.

5. Discussion

A specific feature of the near-infrared photoluminescence of bismuth inclusions in all samples under study is the increase of the 1420-nm wavelength peak intensity with the increase of temperature (Fig. 4), which is accompanied by slowing down of the decay process. Luminescence decay follows a bi-exponential function, with the time constants being weakly dependent on temperature with a significant variation of the pre-exponential factors ratio.

The described behavior of the luminescence spectra is in agreement with that found for bismuth-doped bulk silica glasses [11]. According to the three-level energy diagram proposed and described in [11], the growth of the luminescence intensity in the 1420-nm wavelength band at higher temperatures is associated with the increase of the photo-excited electron transition rate to a meta-stable level of the bismuth cluster.

#227047 - $15.00 USD Received 18 Nov 2014; revised 19 Jan 2015; accepted 22 Jan 2015; published 6 Feb 2015

A decrease in the 1420-nm wavelength luminescence peak on heating to the highest temperatures is one of the distinctive features of bismuth clusters in fluorinated silica. This we attribute to a possible reconfiguration of some bismuth clusters in the fluorine-containing silica network heated to a temperature of ~900 K. Last mentioned could take place due to a greater porosity of the fluorine-modified silica network. Reconfiguration of clusters is accompanied by an irreversible loss of their luminescence capability. Experiments confirmed the irreversible loss of the luminescence properties of bismuth in the sample annealed at 900 K without notable changes in the decay pattern. It should be noted that in fluorine-free silica-core fibre, no degradation of this luminescence band intensity resulting from annealing at 900 K is detected.

The complicated luminescence-decay kinetics observed at elevated temperatures indicates that at least two types of bismuth clusters contribute to this process. In such a case temperature increase causes an increase of the relative contribution of a longer-living component (Fig. 6 (b)). It should also be noted that in all samples the temperature increase affects the intensity but not the shape of the spectral band (Fig. 4). One can conclude that bismuth luminescence is caused by two similar types of clusters having the same shapes of emission spectra but different luminescence lifetimes. Following the cluster model discussed in [4], it may be assumed that fast and slow luminescence is associated with bismuth aggregates of different sizes. This assumption is supported by the fact that bi-exponential luminescence decay is most tangible in the sample with the greatest content of fluorine in the core glass. This also agrees with the fact that higher porosity of the glass network leads to preferable formation of bismuth clusters of larger sizes. Why bismuth clusters of larger sizes have a longer luminescence lifetime is a question for a separate investigation beyond the scope of the present article.

An alternative explanation for the bi-exponential pattern of the luminescence decay may be the contribution to luminescence of bismuth clusters of a similar size, but located in voids of different types present the fluorine doped silica network. The voids are characterized by two different nearest environments.

Now let us consider the results of experiments on the influence of dissolved hydrogen and deuterium molecules on luminescence properties of the samples under study. It is known [19, 20] that the maximum concentration of hydrogen molecules dissolved in silica reaches ~10^{22} cm^{-3}. This corresponds approximately to the density of voids which are capable of housing a hydrogen molecule. The typical size of such a void is about 10 Å, while the linear size of a hydrogen molecule is ~2.5 Å [21]. As shown in [20], full saturation of silica with hydrogen does not take place even at pressures of about 75 kbar. Hence we can conclude that at pressures not significantly exceeding 100 bar, one void would contain no more than one hydrogen molecule.

According to our measurements, hydrogen dissolved in the glass starts to cause a significant impact on luminescence decay at temperatures greater than ~120 K, which is close to the excitation temperature for hydrogen molecules' rotational degrees of freedom. Whereas the motion of hydrogen molecules inside silica glass is known to keep rotational degrees of freedom [16], one can conclude that interaction between an excited bismuth cluster and a hydrogen molecule starts to occur as soon as the molecule stays in an excited rotational state.

We suppose that as a result of such interaction, the energy of the excited bismuth cluster is transferred to a vibrational degree of freedom of a molecule (not excited at any temperature in the current experiment) and further on to vibrations of the silica network by means of subsequent contacts. In fact, according to our model, hydrogen molecules act as extra bridges for nonradiative transfer of excitations from activated bismuth clusters to the glass. The current model allows one to find a simple explanation for the revealed deviation of luminescence decay from the exponential function at temperatures greater than ~120 K (Fig. 10(b)). Whether an excited bismuth cluster is quenched by an H_2 molecule probably depends on the proximity of the molecule to the cluster and whether its vibrational degree of freedom

#227047 - $15.00 USD Received 18 Nov 2014; revised 19 Jan 2015; accepted 22 Jan 2015; published 6 Feb 2015

remains excited as a result of the previous interaction; that is, it is dependent on the process prehistory. As a result, the quenching process becomes non-Markovian, which naturally leads to non-exponential luminescence decay (Fig. 10(b)) [22]. From this viewpoint, it is easy to qualitatively explain the increasing quenching rate in a gas-saturated fibre with increasing temperature (Fig. 11(a, b)). Indeed, the higher the temperature, the greater the rate of random walking of a molecule inside a void, which in its turn enhances the probability of encountering an excited bismuth cluster.

Hydrogen in-diffusion (Fig. 7 (a)) and subsequent heating (Fig. 9 (a)) cause a monotonic-intensity decrease of the steady-state luminescence band peaking at a wavelength of 1420 nm. Similar changes in luminescence spectra are observed in the case of deuterium. The observed dependences on temperature testify to a great significance of the dissolved molecules' rotational degrees of freedom for collisional quenching of the excited bismuth clusters. The smaller impact of deuterium on the quenching rate (Fig. 12(a)) is due to the greater mass and rotational inertia of this molecule and hence a smaller rotation frequency (a gap in the rotation energy diagram).

Heating in hydrogen ambience at high temperatures (> 570 K) leads to the appearance of a dip in the luminescence spectrum at a wavelength of 1380 nm, which is associated with the absorption increase caused by the formation of Si-OH groups in the glass. This effect is irreversible.

6. Conclusion

Silica-based optical fibres with a fluorine-doped core revealed novel properties of bismuth inclusions in silica. The first thing observed is a multiplicity of bismuth inclusions. Such a multiplicity is evident from the variations in the visible and UV absorption spectra and depends on fluorine content. Whereas the silica glasses used in our experiments are differentiated by fluorine content only, the multiplicity of bismuth embedment is of a topologic nature and is apparently associated with bismuth cluster sizes.

A peculiarity of the near-infrared luminescence band centred at the 1420-nm wavelength is an anomalous growth of this band's luminescence intensity and lifetime with increasing temperature. Strongly fluorinated glass fibre features tangibly bi-exponential luminescence decay at the temperature of liquid nitrogen.

As a result of hydrogen loading, all luminescence decay curves start to follow Kohlrausch functions (stretched exponents), which are most strongly manifested at elevated temperatures. The experiments confirm that hydrogen- and deuterium-loading leads to luminescence quenching. Other conditions being equal, hydrogen has a stronger effect than deuterium. We showed that a mechanism responsible for luminescence quenching is the energy transfer from an excited bismuth cluster to vibrational degrees of freedom of migrating hydrogen or deuterium molecules with subsequent energy dissipation via vibrations of the silica network. Of great importance for this process is an excited state of the interstitial molecule with regard to the rotational degrees of freedom.

The experimental data obtained provide additional evidence for a cluster rather than a point defect model for bismuth defects in silica being responsible for near-infrared luminescence.

Acknowledgments

The authors are grateful to Dr. Yu. K. Chamorovskij and Messrs. A.A. Kolosovskii, V.V. Voloshin, and I.L.Vorob'ev for their invaluable contribution to the fibre fabrication.

The research is financially supported by the Russian Scientific Foundation (Project 14-13-01422).

#227047 - $15.00 USD Received 18 Nov 2014; revised 19 Jan 2015; accepted 22 Jan 2015; published 6 Feb 2015